Wang *et al. Hepatoma Res.* 2025;11:10
DOI: 10.20517/2394-5079.2024.129

Hepatoma Research

Original Article

Open Access

The interaction effect between key autophagy-related biomarkers and HBV/HCV infections on the survival prognosis of hepatocellular carcinoma

Ruiping Wang[1], Hui Guo[1], Xiaoni Kou[1], Rongrong Chen[2], Rongqiang Zhang[2], Jingtao Li[1]

[1]Ward II of Hepatology Hospital, Affiliated Hospital of Shaanxi University of Chinese Medicine, Xianyang 712000, Shaanxi, China.
[2]School of Public Health, Shaanxi University of Chinese Medicine, Xianyang 712046, Shaanxi, China.

Correspondence to: Prof. Rongqiang Zhang, School of Public Health, Shaanxi University of Chinese Medicine, Shiji Ave., Xi'an-Xianyang New Ecomic Zone, Xianyang 712046, Shaanxi, China. E-mail: zhangrqxianyang@163.com; Prof. Jingtao Li, Ward II of Hepatology Hospital, Affiliated Hospital of Shaanxi University of Chinese Medicine, No. 2, Weiyang West Road, Xianyang 712000, Shaanxi, China. E-mail: dr_lijingtao@163.com

How to cite this article: Wang R, Guo H, Kou X, Chen R, Zhang R, Li J. The interaction effect between key autophagy-related biomarkers and HBV/HCV infections on the survival prognosis of hepatocellular carcinoma. *Hepatoma Res.* 2025;11:10. https://dx.doi.org/10.20517/2394-5079.2024.129

Received: 22 Oct 2024 **First Decision:** 2 Dec 2024 **Revised:** 21 Feb 2025 **Accepted:** 27 Feb 2025 **Published:** 21 Mar 2025

Academic Editors: Dar-In Tai, Nan Li **Copy Editor:** Ting-Ting Hu **Production Editor:** Ting-Ting Hu

Abstract

Aim: This study aimed to investigate the prognostic and diagnostic value of autophagy-related genes (ATGs) in hepatocellular carcinoma (HCC).

Methods: The expression profiles of differentially expressed ATGs (DEAs) were extracted from The Cancer Genome Atlas (TCGA), Human Protein Atlas (HPA), International Cancer Genome Consortium (ICGC), and TIMER databases. The biological functions and enrichment pathways related to the DEAs were determined. In the TCGA training cohort, univariate Cox regression was used to define HCC subtypes, and prognostic ATGs were submitted to LASSO Cox analyses to generate overall survival (OS), progression-free survival (PFS), disease-free survival (DFS), and disease-specific survival (DSS)-related models. The ICGC validation cohort [the Liver Cancer-RIKEN JP (LIRI-JP)] was used to examine the predictive models. The Kaplan Meier, nomogram, and receiver operating characteristic (ROC) analyses were used to confirm the accuracy of the prediction. The relationship between prognostic signature and clinicopathologic parameters, genetic alterations, tumor microenvironment, and subcellular location annotation was also examined by multiple databases.

Results: A total of 50 DEAs were identified and enriched in autophagosome membrane, programmed cell death,

and PI3K-Akt signaling pathways. *BIRC5*, *GAPDH*, *FKBP1A*, and *RAC1* were significantly correlated with poor prognosis and were identified to be independent predictors for HCC OS and DSS (HR > 1.8, $P < 0.05$). The risk score of prognostic models has confirmed that *BIRC5* was an independent prognostic factor. The calibration curve has validated the accuracy and reliability of the nomogram for survival years, as well as ICGC validation using the same risk models. *BIRC5* may influence the mortality of hepatitis B and C patients. Immunohistochemistry showed that *BIRC5* protein was moderately expressed in HCC and may influence tumor detection and genetic mutations. High amplification of *BIRC5* may inhibit the immune infiltrates as CD4 T cells, macrophages, and neutrophils.

Conclusion: *BIRC5* is overexpressed in HCC tissues, indicating a poor prognosis that could be a new prognostic biomarker, treatment target, and diagnostic signature for HCC.

Keywords: Hepatocellular carcinoma, autophagy, *BIRC5*, prognosis, biomarker

INTRODUCTION

The international Agency for Research on Cancer (IARC) reported that more than 19.3 million novel tumor cases and 10 million cancer-related deaths occurred all around the world in 2020[1]. Hepatocellular carcinoma (HCC) is the third leading cause of cancer-related deaths and the sixth in terms of incidence among malignancies[2], accounting for 90% of all primary liver cancers[3,4]. Its pathological changes are determined by epigenetic and genetic alterations, including genomic insertions, mutations, and deletions[5,6]. Globally, HCC has become a serious public health issue, with rising morbidity and mortality. As reported, the 5-year survival rate of HCC patients only reached 18% in the United States[7]. Every year, more than 850,000 new instances of liver cancer are diagnosed globally, with 782,000 fatalities[8]. It is estimated that by 2030, globally, HCC-associated mortality will reach 1 million cases annually[9]. Hepatitis B virus (HBV), Hepatitis C virus (HCV), and alcoholism are all substantial risk factors for HCC development, and they are all linked to a poor prognosis and high aggressivity[10,11]. Tumors are heterogeneous and drug-resistant, and despite the advances in therapy, such as anti-viral drugs, surgical interventions, immunotherapeutic agents, and targeted therapies, HCC remains a formidable threat and a great public health challenge[12]. Therefore, it is crucial to identify suitable prognostic and diagnostic biomarkers for early HCC stages to guide effective treatment.

Autophagy is a highly conserved intracellular degradation mechanism, which is required for cellular homeostasis, protein quality management, and pathogen defense as well[13]. Autophagy plays various roles in the maintenance of liver homeostasis by eliminating damaged mitochondria and promoting cellular processes that preserve genomic stability, prevent malignant transformation, and mitigate chronic cell damage[14,15], especially in the early stages of tumorigenesis[16]. Under the regulation of autophagy-related genes (ATGs), the autophagy degradation process delivers basic nutrients and energy to liver cells[12,16], all of which are commonly interrupted during carcinogenesis and cancer treatment[13]. Currently, preclinical findings have offered circumstantial evidence of a link between autophagy-related activities and HCC prognostic outcomes[17]. For instance, Fang *et al.* reported that autophagy suppression reduces HCV replication in human hematoma cells[18]. In hepatoma cells, autophagy-related 5 (ATG 5) siRNA inhibits autophagy while increasing norcantharidin-induced apoptosis[19]. Suppressed autophagy elevates the levels of the autophagy protein p62, which stimulates the production of the Nrf2, which promotes liver fibrosis and liver cancer progression[5,20] while also lessening HCC cell sensitivity to sorafenib[21]. Over recent years, the ATG signature has been developed to predict prognosis in diverse types of tumors, such as resected breast tumors [22], pancreatic cancer[23], and glioma[24]. AFP, VEGF, and ANG-2 were indicated as prognostic biomarkers for HCC by the European Association for the Study of the Liver (EASL), whereas Keratin-19 and EpCAM were presented as prognostic options for their link with poor prognosis outcomes for HCC

patients[17,25]. Nevertheless, the predictive efficacy and diagnostic significance of ATG signature have not been examined for HCC.

In this study, we constructed signatures of ATGs through RNA expression levels of differentially expressed autophagy-related genes (DEAs) related to HCC, which were obtained from The Cancer Genome Atlas (TCGA) cohort and the Human Autophagy Database (HADb). Notably, the autophagy-related prognostic signature related to HCC survival prediction was also determined using clinical prognosis prediction models according to the risk score cutoff value. Following that, the International Cancer Genome Consortium (ICGC) dataset [the Liver Cancer-RIKEN JP (LIRI-JP)] was used to verify the HCC prognostic signature. Notably, the models exhibit promising prognostic ability and might be used to help HCC patients make healthcare decisions.

METHODS

Data source and processing

Transcription profiling RNA-seq data, along with the corresponding clinical data for 374 HCC samples and 50 adjacent normal tissues, were acquired from the "TCGA-LIHC" dataset in the TCGA public resource portal (https://tcga-data.nci.nih.gov/tcga/)[26].

Meanwhile, the samples extracted from the TCGA cohort were used as the training group, and those from the ICGC (http://dcc.icgc.org/releases/current/Projects) portals served as the validation cohort, which provided 202 normal tissues and 243 HCC tissues.

The HADb (https://autophagy.lu/v1/clustering/), a specific database for conserving genes related to human autophagy, yielded a total of 232 ATGs[27].

Notably, raw data were filtered to remove duplicated and missing findings. First, raw data were normalized by $\log_2$(TPM +1) transformation using "RMA" (version 4.1.3) in R. Then, 19,654 protein-coding genes were annotated. The "affy" package was used to perform robust multi-array average normalization and quantile normalization on the microarray data.

Identification and functional enrichment analysis of DEGs in HCC

The R package "DESeq2" was used to identify the differentially expressed genes (DEGs) related to HCC, $|\log_2 FC| > 1$, and false discovery rate (FDR) < 0.05 were deemed significant, and the *P* value adjusted by FDR.

GO and KEGG analyses performed functional and enrichment pathways related to DEGs. KEGG is a massive database that contains information about chemical, genetic, and system activities, while GO functional annotation is a database for characterizing and defining input genes as well as protein activities in numerous species[28].

Identification of differentially expressed ARGs

The expression profile of DEAs between HCC cases and normal controls was extracted from the HADb database and the TCGA transcription profiling data. The Wilcoxon test was applied to evaluate the significance of the variation in gene expression, with a significant threshold of $|\log_2 FC| > 1$ and FDR < 0.05. The Kruskal-Wallis test was utilized to compare gene expression significances in various tissues.

To predict protein functions, the STRING (version 11.5, https://string-db.org/) database was used, with a combined score > 0.6 as the criterion. Cytoscape (version 3.8.0, https://cytoscape.org/) was applied to

display the protein-protein interaction (PPI) network[29]. GO and KEGG analyses were completed using "GOplot" and "ClusterProfiler" packages in R to execute the enriched ontologies, biological features, and disease pathways.

Prognostic significance of DEAs in HCC

Overall survival (OS), disease-free survival (DFS), progression-free survival (PFS), and disease-specific survival (DSS) for 374 HCC samples from the TCGA-LIHC dataset were analyzed to assess whether DEAs were associated with prognostic significance in HCC patients. Using Kaplan-Meier survival curves based on the median risk score, as well as hazard ratio (HR) values with a 95% Confidence Interval (95%CI) and log-rank $P < 0.05$, the HCC patients were categorized into high-risk ($n = 185$) and low-risk ($n = 185$) groups.

Construction of the risk signature for survival prediction of HCC patients

The prognostic risk signature was produced using a LASSO Cox regression model and the R packages, "glmnet" and "survival", to avoid false-positive outcomes and overfitting of the prognostic signature. Then, the prognostic relevance of OS-, DFS-, PFS-, and DSS-related prognostic signatures of HCC was determined using univariate and LASSO Cox regression analyses (FDR < 0.05). Running cross-validation 1,000 times yielded the best value for the penalization coefficient lambda (λ) computed in multivariate Cox regression, with the risk score = $\sum_{i=1}^{n} Coefi \times Exprei$. Following that, using the Kaplan-Meier survival method, survival curves were generated to represent the clinical outcomes of high-risk ($n = 185$) and low-risk ($n = 185$) patients in HCC. The prognostic performance of the four risk models (OS-, DFS-, PFS-, and DSS-related HCC risk models) was evaluated using time-dependent receiver operating characteristic (ROC) analyses at 1-year, 3-year, and 5-year follow-up, which could examine the specificity and sensitivity of DEAs in outcome prediction.

Establishment of the prognostic signature

Hence, four DAE signatures were optimized based on the coincidence of two prognostic models, OS and DSS. Then, to determine whether four DEA signatures, age, gender, pathological grade, and tumor types were independent prognostic factors for HCC tumorigenesis, all factors were included in the parameters of univariate and multivariate Cox regression. HR and 95%CI were used for the calculation of prognostic signature, and $P < 0.05$ was deemed significant. The "rms" in the R package was applied to develop a nomogram that was utilized to validate the patients' OS, PFS, DSS, and DFS probability as well as the prognostic value. The C-index was generated through "survcomp" to assess the accuracy of the Cox regression models in predicting the prognostic outcomes of HCC patients (normal: 0.50-0.70, medium accuracy: 0.71-0.90; high accuracy: > 0.90). Notably, the calibration curve, which presents the areas under the curve (AUC) values of HCC patients at 1-, 2-, 3-, and 5-years, was constructed and utilized to test the accuracy and reliability of the nomogram.

Validation of the prognostic signature

To validate the efficiency of prognostic signatures, LASSO-Cox regression analysis has been established to calculate the optimal score of prognostic signatures. The clinical trait data, LIRI-JP, related to prognostic signature were retrieved from the ICGC cohort for HCC. The risk score was generated using the same algorithm used in the TCGA training cohort, and the mRNA expression levels of the prognostic signature were standardized using the "scale" function. Using the optimal cutoff value of Kaplan-Meier analysis obtained from the ICGC cohort, a total of 243 HCC patients were separated into two groups: high-risk and low-risk. Then, a log-rank test was performed to compare survival curves between the two groups. Additionally, the specificity and sensitivity of the prognostic signature in predicting outcomes at 1, 3, and 4 years were demonstrated using ROC curve analysis.

Crosstalk between BIRC5 expression and hepatitis B and C

Hepatitis B and C are major pathogenic factors in HCC. Clinical data from 372 HCC patients in the TCGA cohort were analyzed to better understand the influence of the interaction between prognostic signature expression and hepatitis B and C on survival outcomes in HCC. Patients were divided into infected (n = 60) and uninfected (n = 312) groups. The individuals were also classified as HCV infected (n = 19) and uninfected (n = 353). Based on the median signature score, patients with hepatitis B or C ere further categorized into high-and low-risk groups, as were the uninfected patients. The effect of high and low expression of a signature on survival and prognosis were also evaluated using the Log-rank test with hepatitis C data. Kaplan-Meier curves were constructed using the "survminer" package in R, and survival predictions were made using the "survival" R package.

Expression of prognostic signature

To compare the levels of signature expression in normal tissues and malignancies, the GEPIA (http://gepia.cancer-pku.cn/) database, which integrates TCGA normal and GTEx data, was used to investigate the mRNA expression of the prognostic signature, setting the threshold as $|\log_2 FC| > 1$ and $P < 0.05$. The "PATHOLOGY" and "TISSUE" modules of the Human Protein Atlas (HPA, https://www.proteinatlas.org/) were employed to examine protein spatial distribution at the cellular and subcellular levels in normal tissues compared to HCC tissues[30].

Association between signature, genetic alterations, and immunotherapy biomarkers

The c-Bioportal (https://www.cbioportal.org/) database presently contains multidimensional cancer genomics data for approximately 5,000 samples across 20 cancer types[31]. The c-Bioportal database discovered gene mutations, copy number variations (CNV), and mRNA expressions among the genetic alterations for prognostic signature. The "OncoPrint" tab presented a trademark summary of genetic changes discovered in each HCC sample. Tumor mutational burden (TMB) is a new cancer characteristic that measures the number of somatic mutations per 1 million bases in a tumor[32]. Surprisingly, neoantigens produced by elevated TMB trigger spontaneous antitumor immune responses and potentially predict responses to cancer immunotherapies[33,34]. In a variety of malignancies, microsatellite instability (MSI) is an efficient prognostic biomarker and immunotherapeutic response predictor[35]. The SangerBox database (http://sangerbox.com/) was then used to explore associations between signature levels and TMB, MSI, and neoantigens in malignancies[34], with statistical significance, determined as a $P < 0.05$.

Tumor immune microenvironment and subcellular location annotation

Six types of immunological infiltrates - B cells, CD4 T cells, CD8 T cells, macrophages, neutrophils, and dendritic cells - were examined using the "SCNA" module in the TIMER database (http://timer.cistrome.org/)[36]. Box plots were utilized to illustrate the distribution of each immune cell type across different mutation states in HCC, and the Wilcoxon rank test ($P < 0.05$) was applied to assess differences in infiltration levels in each category. The HPA database was utilized to evaluate the signature expression of proteins in all cell lines (n = 69). Based on available gene characterization data from the HPA, each subcellular location was immunofluorescently annotated, and immunohistochemistry (IHC)-stained tissues were graded according to the reliability of the analyzed protein expression[30].

Statistical analysis

The statistical analysis was performed using the R software (v4.1.3) and GraphPad Prism (v9.2). To predict and validate the prognostic significance of the autophagy-related risk signature, the "survival ROC" and "rms" R packages were employed. For each of the biomarkers and particular combinations, the diagnostic performance was examined and compared using ROC analysis. Qualitative data were given as a percentage, whereas quantitative data were expressed as mean ± standard deviation ($\bar{x} \pm s$). Differences between groups

were evaluated using the Student's *t*-test. Using the "survival" in R, the Kaplan-Meier curve and log-rank test were performed to characterize the connection between survival time and survival probability for the high-risk and low-risk groups. $P < 0.05$ denoted significance.

RESULTS

Identification and functional annotations of DEGs in HCC

A total of 2,915 DEGs were screened from HCC tissues and normal controls [Figure 1A and B]. Of these, 2,371 upregulated DEGs (81.34%) were considerably enriched in phagosomes, non-alcoholic fatty liver disease (NAFLD), mRNA catabolic processes, and pathways involved in oxidative phosphorylation, and bacterial invasion of epithelial cells. In contrast, 544 downregulated DEGs (18.66%) were significantly enriched in cellular amino acid metabolism, chemical carcinogenesis, small molecule catabolic processes, pathways related to epoxygenase P450, and the PPAR signaling pathway [Figure 1C].

Identification of differentially expressed ARGs

A total of 50 DEAs were identified, consisting of 42 upregulated and 8 downregulated genes [Figure 2A]. The largest fold differences were observed in *BIRC5* ($Log_2FC = 2.7$) and *SPNS1* ($Log_2FC = -2.5$). Most of these DEAs showed significant associations with the MAPK3 and TP53 proteins in the PPI network [Figure 2B], which were also primarily enriched in the lysosome, autophagosome membrane, and endoplasmic reticulum, where they were mainly involved in processes such as autophagy, programmed cell death, and the regulation of phosphate metabolism [Figure 2C]. Additionally, they played roles as structural constituents in catalytic activities, enzyme regulator activities, and protein domain-specific binding. Meanwhile, KEGG analysis revealed that these DEAs were predominantly enriched in pathways related to apoptosis, HCC, autophagy in animals, and signaling pathways like cancer, PI3K-Akt, and NOD-like receptor [Figure 2D].

Prognostic significance of DEAs in HCC

A total of 26 DEAs were linked to a poor HCC OS [Figure 3A], whereas 15 DEAs were substantially related to a poor HCC DSS [Figure 3B]. Then, *BIRC5*, *FKBP1A*, *GAPDH*, and *RAC1* (HR > 1.8) were identified as potential independent risk factors for OS and DSS models that were substantially associated with poor prognosis for HCC [Figures 4 and 5].

Risk signature for survival prediction of HCC patients

The LASSO Cox models revealed that 18 potential prognostic ATGs were correlated with HCC OS when the minimum λ value was 0.0195 [$P < 0.05$, Figure 6A-C]. The K-M method showed that the high *BIRC5* expression group had worse OS [Figure 6D], implying that a high risk score is an adverse prognostic factor ($P < 0.05$). Based on the combined risk score constructed from the OS-related LASSO Cox models, *BIRC5* emerged as the best candidate for a risk-related prognostic signature. The AUC values for the four models, predicting 1-, 3-, and 5-year survival outcomes, demonstrated strong predictive performance [Figure 6E].

Construction of the prognostic signature

Univariate and multivariate Cox models were constructed for the screened significant signatures. The forest plots determined by Univariate Cox showed that *VEGFA*, *SQSTM1*, *FKBP1A*, and *BIRC5* are potential prognostic signatures related to HCC OS [Figure 7A]. However, multivariate Cox analyses showed that only *BIRC5* was filtered as an independent prognostic signature for the HCC OS [Figure 7B]. Increased risk scores in patients were associated with shorter survival times and higher mortality. The nomograms were used to calculate the total scores predicting 1-, 2-, 3-, and 5-year survival probabilities by aggregating the scores for each HCC patient. The C-index for OS [Figure 7C] was calculated as 0.682, 0.631, 0.686, and 0.634, respectively. Notably, the prediction accuracy improves as the calibration curve approaches the

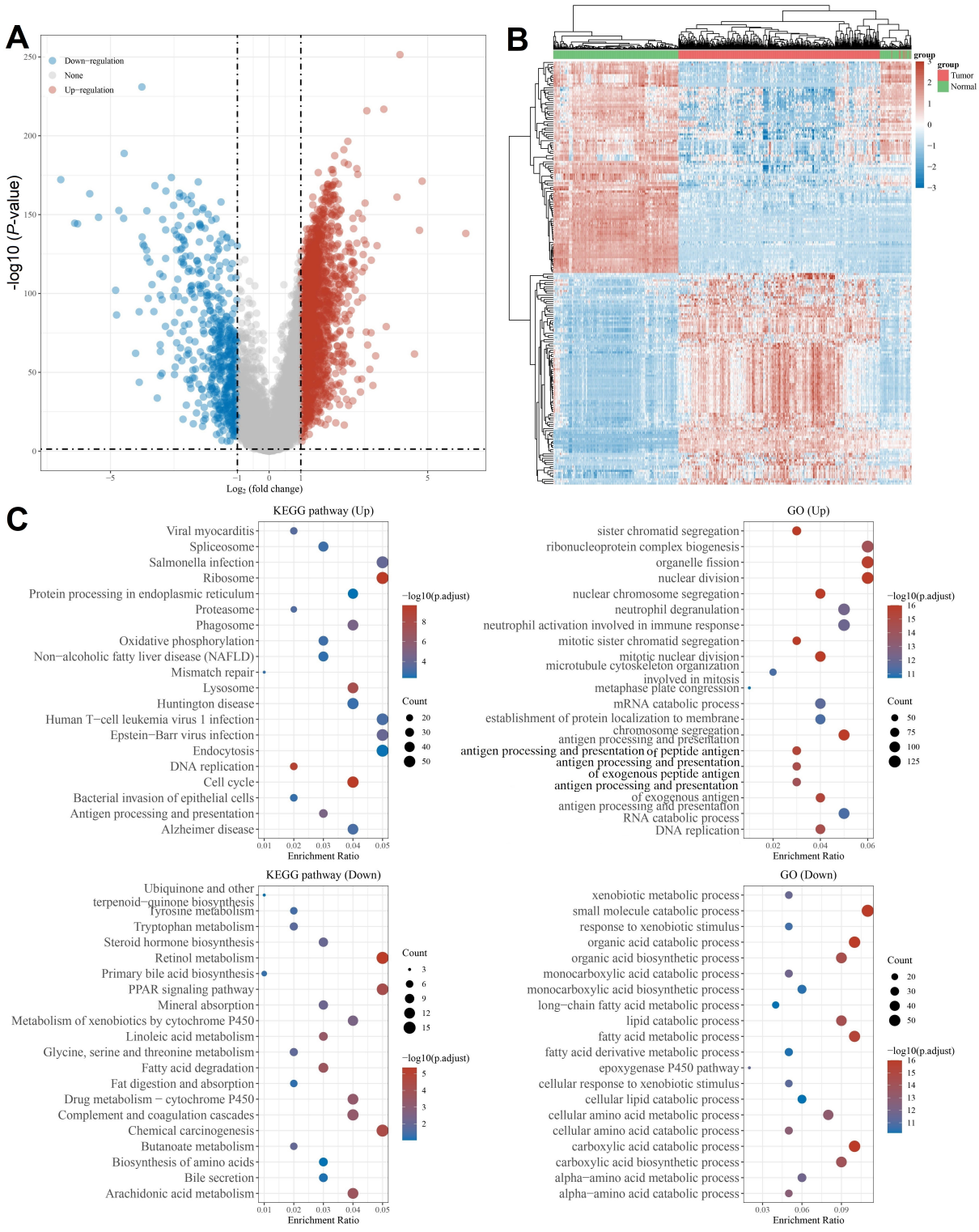

Figure 1. The identification of DEGs for HCC. (A) Volcano plot; (B) Heatmap; (C) GO and KEGG enrichment analysis among up- and downregulated DEGs. DEGs: Differentially expressed genes; HCC: hepatocellular carcinoma.

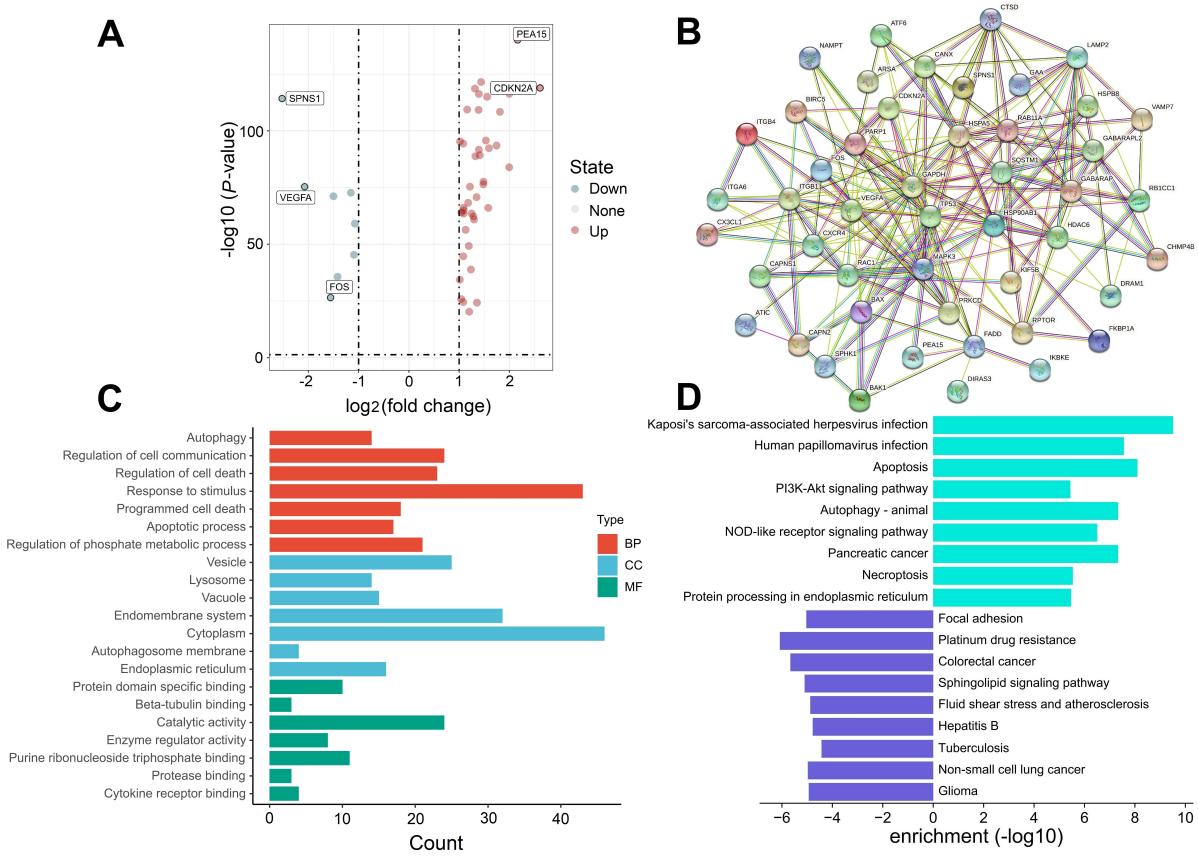

Figure 2. The biological function and enrichment analysis of DEAs in HCC. (A) Volcano plot; (B) PPI network; (C) GO functional analysis; (D) KEGG enrichment analysis. DEAs: Differentially expressed autophagy-related genes; HCC: hepatocellular carcinoma; PPI: protein-protein interaction.

diagonal. The result demonstrated good consistencies between the predicted survival outcomes of the monogram and the observed actual survival outcomes [Figure 7D].

Validation of the prognostic signature BIRC5

The prognostic value and clinical relevance of the signature were subsequently validated in the ICGC external validation cohort. Based on the minimum criteria, a risk model consisting of *TP53*, *ARSA*, *ATIC*, *GAPDH*, *BIRC5*, and *CDKN2A* was established [Figure 8A-C]. A total of 240 HCC patients were divided into two groups: high *BIRC5* expression (n = 120) and low *BIRC5* expression (n = 120). Analysis showed that the low *BIRC5* expression group tended to have a higher mortality rate and worse clinical outcomes compared to the high *BIRC5* expression group [HR = 5.605, Figure 8D]. Furthermore, ROC analysis indicated that the validated model exhibited excellent predictive performance at 1 year (AUC = 0.779), 3 years (AUC = 0.83), and 4 years [AUC = 0.872, Figure 8E]. The results from the ICGC cohort validation were consistent with those observed in the TCGA cohort, suggesting the stability of the validation.

Crosstalk of *BIRC5* expression with hepatitis B and C

To investigate the impact of *BIRC5* expression on the OS of patients with hepatitis B and C, six predictive models were developed. The results revealed that patients with hepatitis B [HR = 1.78, Figure 9A] exhibited poorer prognostic outcomes compared to healthy individuals. Based on median *BIRC5* expression levels, patients with HCC were classified into high and low *BIRC5* expression groups. High *BIRC5* expression was

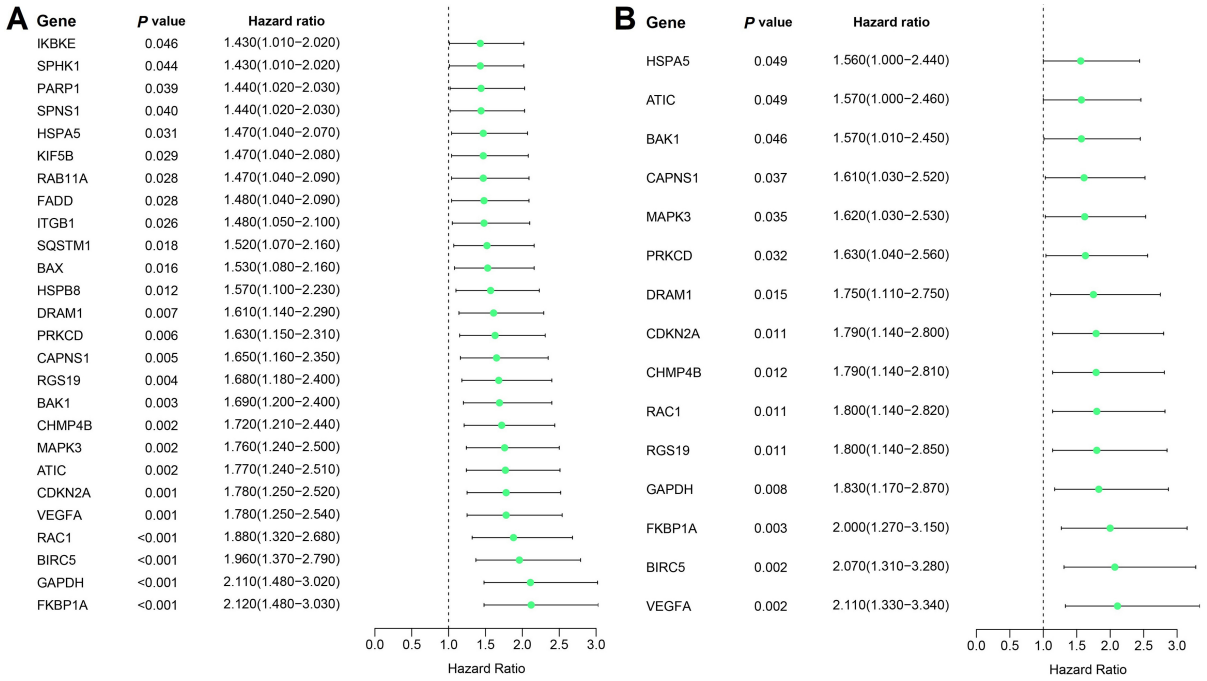

Figure 3. The forestplot determined by the OS-related risk model (A) and DSS-related risk model (B). OS: Overall survival; DSS: disease-specific survival.

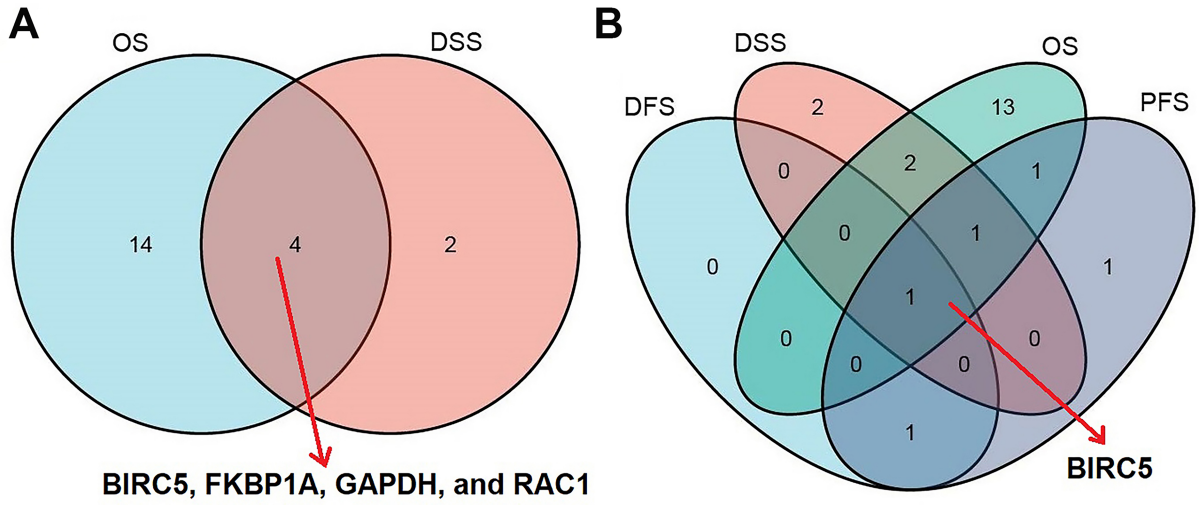

Figure 4. (A) The Venn diagram for the screening of HCC OS- and DSS-related signature genes, including *BIRC5*, *FKBP1A*, *GAPDH*, and *RAC1*; (B) The identification of prognostic signature for OS-, DSS-, DFS-, and PFS-related risk models. HCC: Hepatocellular carcinoma; OS: overall survival; DSS: disease-specific survival; DFS: disease-free survival; PFS: progression-free survival.

associated with reduced survival in hepatitis B patients [HR = 2.63, Figure 9B] and shortened survival in non-infected individuals [HR = 1.47, Figure 9C]. Additionally, patients with hepatitis C [HR = 2.35, Figure 9D] also demonstrated poorer prognostic outcomes compared to healthy individuals. Moreover, elevated *BIRC5* expression was linked to a poor prognosis in both HCV-infected [HR = 2.31, Figure 9E] and non-HCV-infected patients [HR = 1.78, Figure 9F]. These findings suggest that high *BIRC5* expression was a bad prognostic signature, contributing to increased mortality in patients with hepatitis B and hepatitis C.

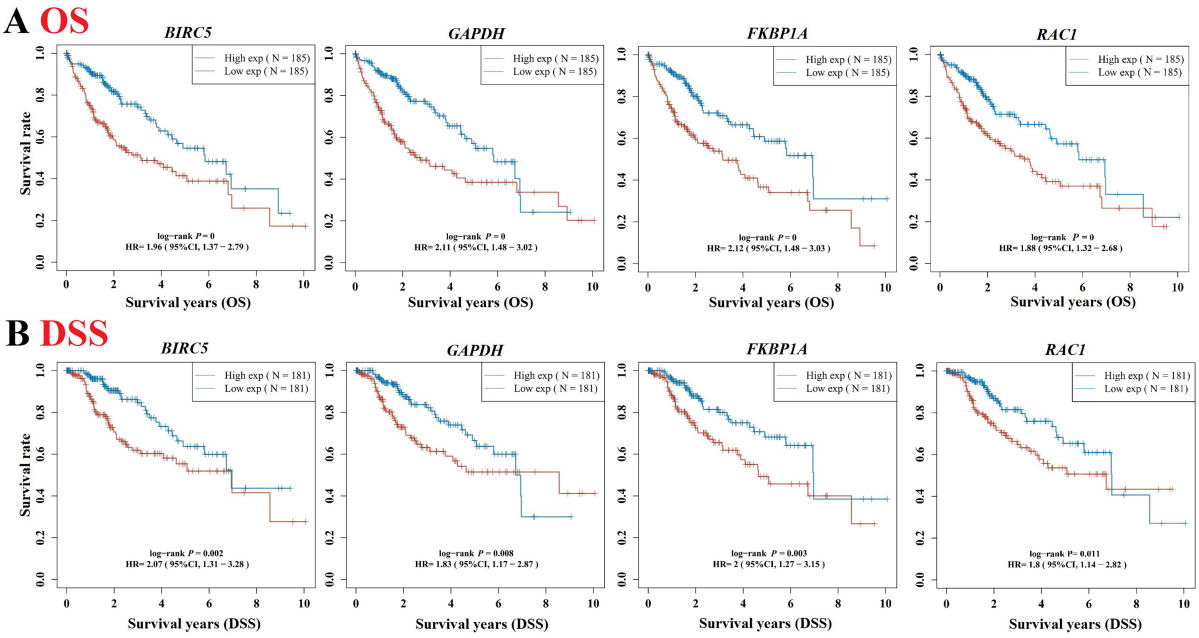

Figure 5. (A) The K-M curves of potential signatures for HCC OS (HR > 1.8); (B) The K-M curves of potential signatures for HCC DSS (HR > 1.8). (*BIRC5*, *FKBP1A*, *GAPDH*, and *RAC1*). HCC: Hepatocellular carcinoma; OS: overall survival; DSS: disease-specific survival; HR: hazard ratio.

BIRC5 expression in normal tissues and HCC tissues

A total of 529 samples were gathered from TCGA and GTEx databases, including 369 HCC cases and 160 normal samples. The results indicated that *BIRC5* protein expression was significantly higher in the HCC group compared to the control group [$P < 0.05$, Figure 10A]. The "Tissue Atlas" from the HPA database illustrated the distribution of proteins across diverse malignant and normal tissues, while the "Pathology Atlas" employed IHC to assess the impact of protein expression on the survival probability of tumor patients. Notably, IHC analysis revealed that *BIRC5* protein expression was moderately elevated in HCC compared to normal tissues, based on cytoplasmic immunoreactivity [$P < 0.05$, Figure 10B].

Association between *BIRC5*, genetic alterations, and immunotherapy biomarkers

As a prognostic signature biomarker in HCC patients, *BIRC5* was implicated with genetic pathology parameters. A total of 1,617 HCC samples from the c-Bioportal database were analyzed, revealing that genomic alterations in *BIRC5* occurred in 4.07% of 369 cases, including 3.79% amplification and 0.27% deep deletion [Figure 11A]. Genetic alterations in *BIRC5* occurred in 2.7% of cases ($P < 0.05$), with the mutation spectrum, cancer type details, and somatic status observed in nearly 100% of the HCC samples [Figure 11B]. Furthermore, the relationship between *BIRC5* and TMB, MSI, and immune neoantigens scores was analyzed. The results revealed that *BIRC5* expression had minimal impact on TMB and neoantigen scores, but it was positively related to MSI in the HCC microenvironment ($P = 0.005$, $R = 0.15$), suggesting that while *BIRC5* may influence tumor detection and genetic mutations, it is not likely to be applicable as a biomarker for immunotherapy [Figure 11C-E].

Tumor immune microenvironment and subcellular location annotation

The underlying relationship between *BIRC5* and immune infiltration levels in the HCC microenvironment was assessed using the TIMER online tool. The results showed a strong positive correlation between *BIRC5* and various immune cell types, including B cells ($R = 0.31$, $P = 1.72 \times 10^{-9}$), CD4 T cells ($R = 0.13$, $P = 0.01$), CD8 T cells ($R = 0.20$, $P = 0$), neutrophil cells ($R = 0.18$, $P = 0$), macrophages ($R = 0.27$, $P = 0.72 \times 10^{-8}$), and

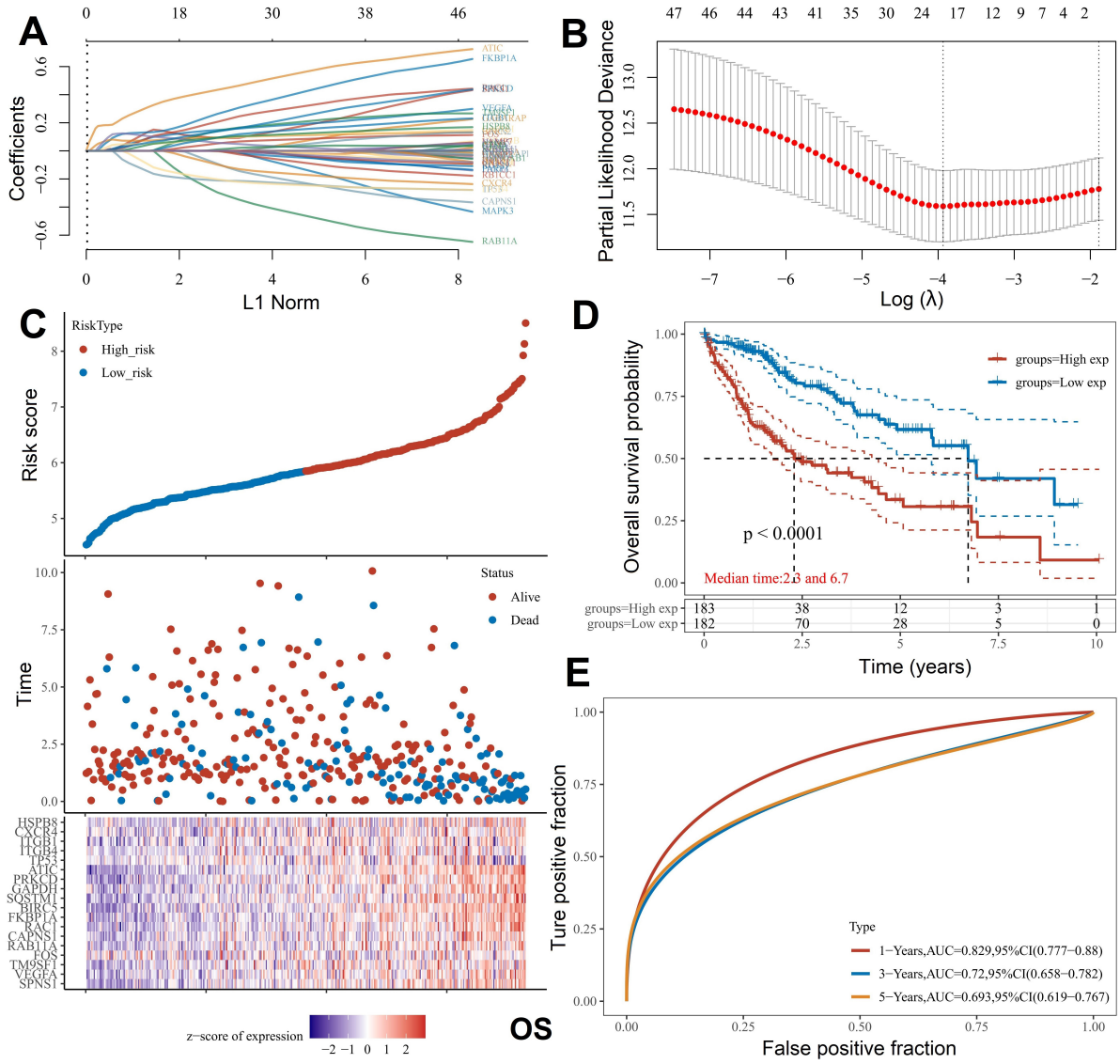

Figure 6. Establishment of the DEAs prognostic classifier according to the OS of HCC based on the TCGA database. (A and B) LASSO Cox regression analysis of ATGs that can significantly affect the HCC OS; (C) The expression of 18 prognosis-related risk genes and the distribution of risk scores and survival status; (D) The overall survival in the high-risk and low-risk groups was analyzed using the K-M method; (E) ROC curves revealed the *BIRC5*'s prediction effectiveness for HCC. DEAs: Differentially expressed autophagy-related genes; OS: overall survival; HCC: hepatocellular carcinoma; TCGA: The Cancer Genome Atlas; ATGs: autophagy-related genes; ROC: receiver operating characteristic.

dendritic cells ($R = 0.27$, $P = 1.75 \times 10^{-7}$) [Figure 12A]. High *BIRC5* amplification was commonly associated with immune infiltrates, such as CD4 T cells, macrophages, and neutrophils [Figure 12B].

For the cell lines summarized, the RNA expression of Hep-G2 in the liver was derived from the "RNA EXPRESSION" module of the HPA database, which reported an expression level of 123.1 nTPM, suggesting low cell line specificity [Figure 13A].

In the "HUMAN CELLS" module analysis, subcellular localization of *BIRC5* was determined using the antibody CAB004270, revealing its presence in the cytokinetic bridge at multiple levels, with expression

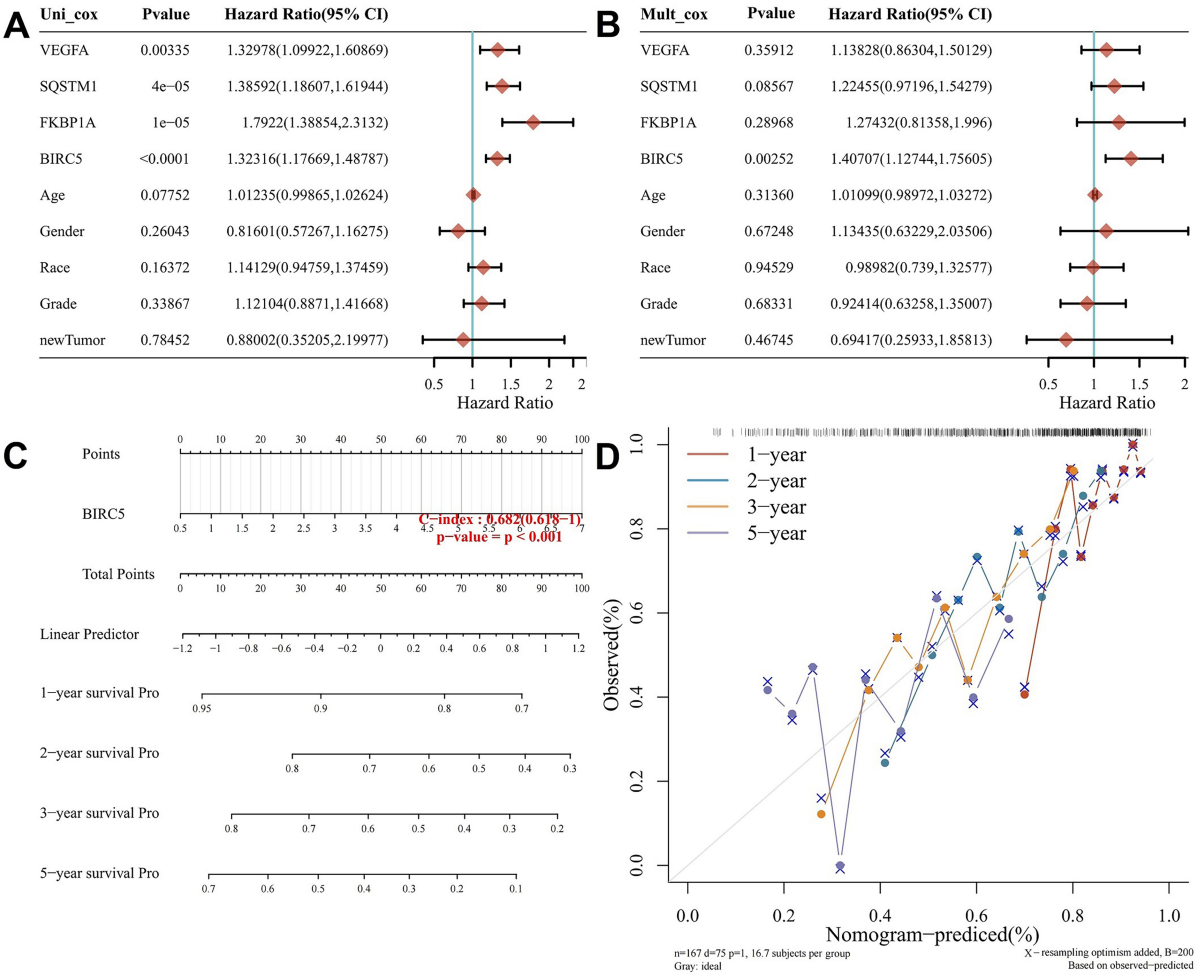

Figure 7. Forest plots and prognostic model affecting OS in HCC. (A and B) Univariate and multivariate Cox regression analysis; (C) A nomogram for predicting 1-, 2-, 3- and 5-year survival rates of HCC patients; (D) The calibration curves for predicting patients' survival at 1, 2, 3 and 5 years. OS: Overall survival; HCC: hepatocellular carcinoma.

values of 139.1 nTPM, 152.6 nTPM, and 150.4 nTPM [Figure 13B-E]. Furthermore, the "SINGLE CELL VARIATION" analysis demonstrated that variations in *BIRC5* transcript expression were closely correlated with the cell cycle, particularly peaking in the G1 phase [Figure 13F and G]. The "SINGLE CELL TYPE" analysis identified *BIRC5* expression across 16 single-cell types in the liver, with particularly high expression in T cells (n = 103, 487.9 nTPM), erythroid cells (n = 91, 261.9 nTPM), and B cells types (n = 520, 174.4 nTPM) [Figure 14A-C].

DISCUSSION

Despite significant advancements in HCC therapy, more than half of Chinese patients remain at high risk of recurrence and metastasis[37]. The effective implementation of precision medicine continues to be a challenge worldwide. Autophagy plays a crucial role in the occurrence and progression of HCC[38-40], maintaining a dynamic equilibrium among genome integrity, cellular metabolism, and homeostasis[41]. Several pathways contribute to HCC metastasis and proliferation, including Wnt/-catenin-mediated autophagy[41,42], the stimulation of epithelial-mesenchymal transition[41,43], and the activation of autophagy via the JNK1/Bcl-2 signaling pathway [41,44]. However, the prognostic significance of aberrantly expressed ATGs

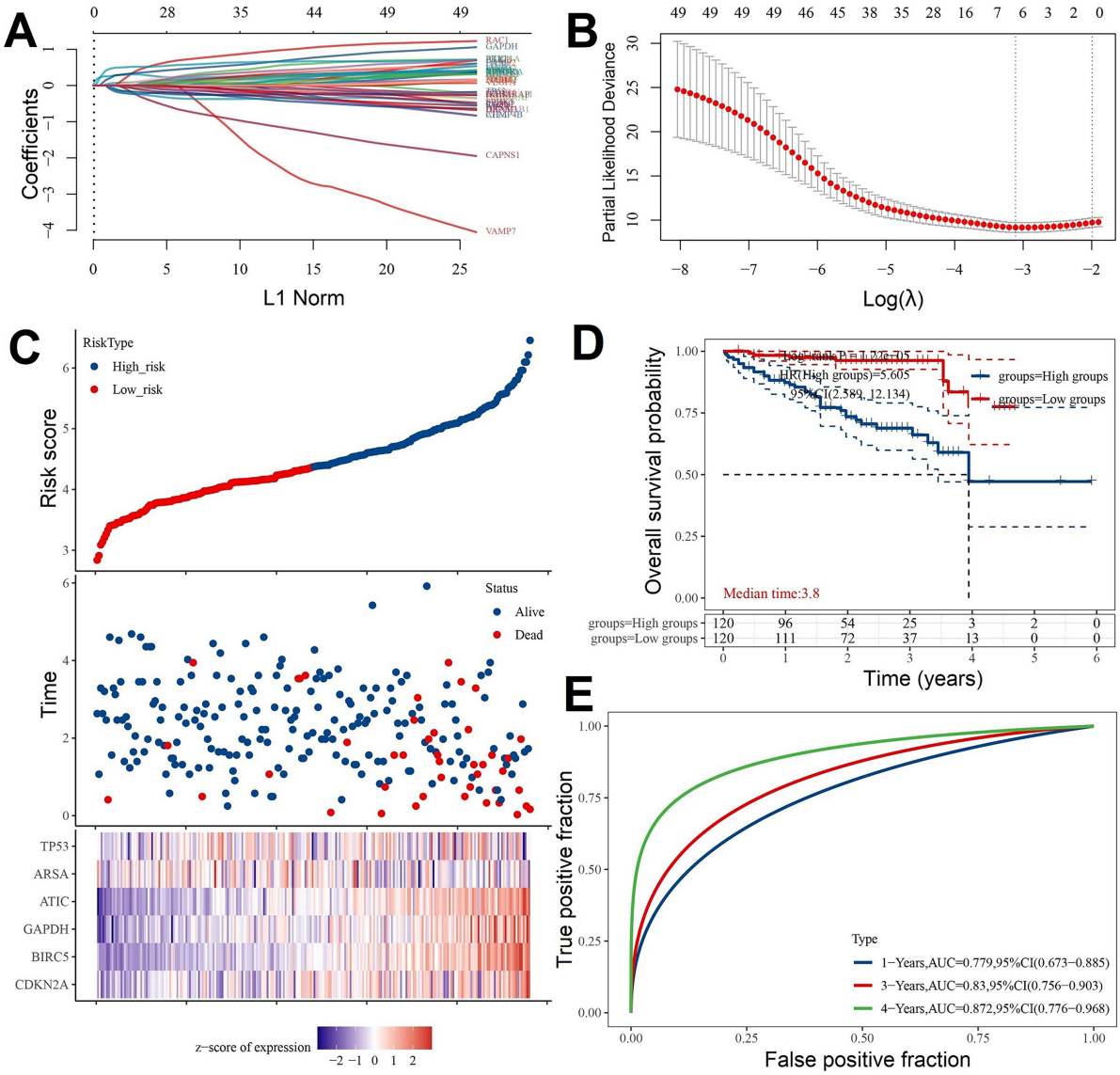

Figure 8. (A and B) The LASSO Cox regression model was built using the six predictive genes discovered in the ICGC training cohort; (C) The expression of six prognosis-related risk genes and the distribution of risk scores and survival status; (D) The overall survival in the high-risk and low-risk groups was analyzed using the K-M method; (E) Based on ICGC cohorts, ROC curves revealed the *BIRC5*'s prediction effectiveness for HCC. ICGC: International Cancer Genome Consortium; ROC: receiver operating characteristic; HCC: hepatocellular carcinoma.

in HCC has not been fully investigated[45]. Therefore, this study aimed to determine an autophagy-related prognostic signature as a potential biomarker for HCC patients.

In this study, high-throughput transcriptomic data and corresponding clinical statistics of HCC patients from the "TCGA-LIHC" dataset were analyzed to identify potential prognostic ATGs. A total of 2,915 DEGs were found to be mainly correlated with autophagy, autophagosome membrane formation, programmed cell death, protein domain-specific binding, and enzyme regulator activities. Additionally, 50 potential ATGs were predominantly linked to several key signaling pathways, including apoptosis, necroptosis, hepatitis B, autophagy (animal), PI3K-Akt, IL-17, Toll-like receptor, and NOD-like receptor pathways. Regarding their prognostic significance in HCC, 26 potential ATGs were strongly associated with poor OS

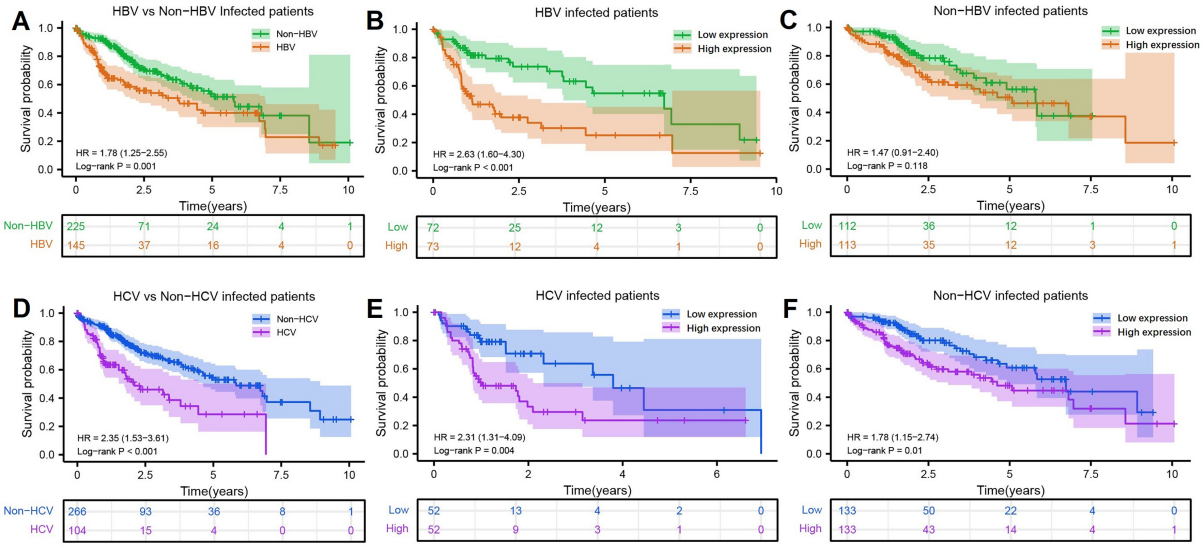

Figure 9. (A) Survival curves for HBV-infected and uninfected patients using Kaplan-Meier analysis. Survival curves for high and low expression of *BIRC5* in HBV-infected group (B) and uninfected group (C) using Kaplan-Meier analysis. Survival curves for HCV-infected and uninfected patients (D). Survival curves for high and low expression of *BIRC5* in HCV-infected group (E) and uninfected group (F) using Kaplan-Meier analysis. HBV: Hepatitis B virus; HCV: hepatitis C virus.

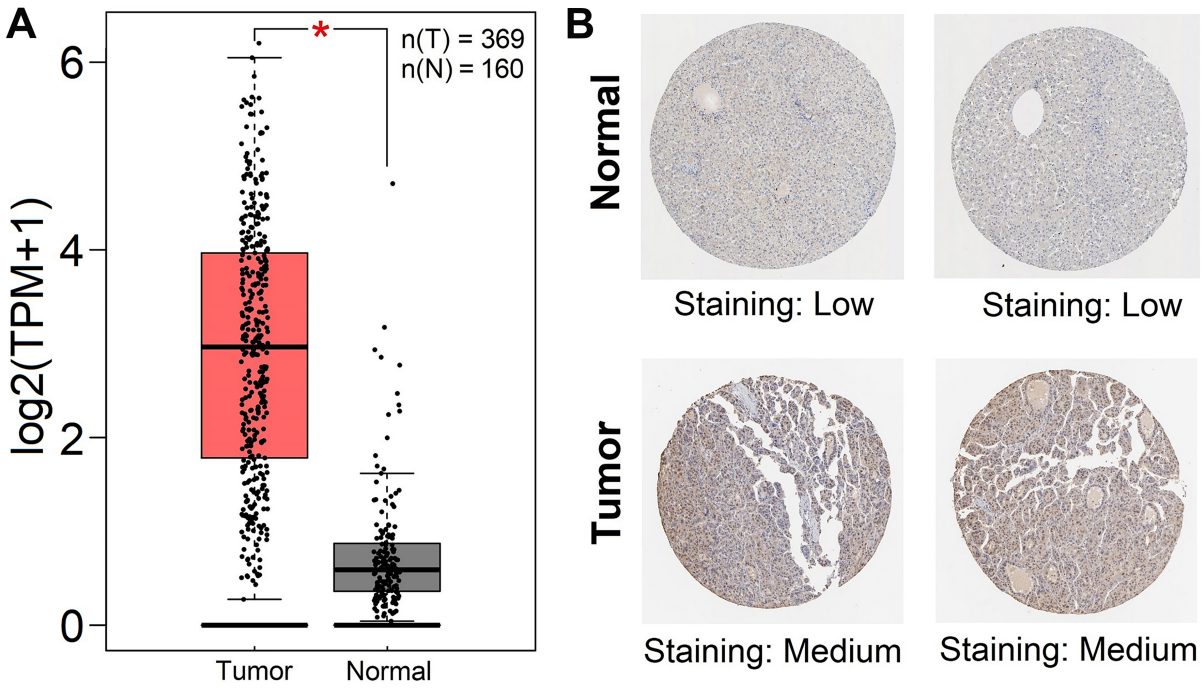

Figure 10. (A) The *BIRC5* mRNA expression in normal tissues compared to HCC tissues from TCGA and GTEx databases; (B) The *BIRC5* protein expression in HCC and normal liver tissue using immunohistochemistry. TCGA: The Cancer Genome Atlas; HCC: hepatocellular carcinoma.

of HCC, while 15 ATGs were linked to poor DSS. However, only four ATGs (*BIRC5*, *FKBP1A*, *GAPDH*, and *RAC1*) were consistently expressed in both OS and DSS analyses. Among them, *BIRC5* was the most upregulated ATG, while *SPNS1* was the most downregulated. Notably, *BIRC5* was found to be highly

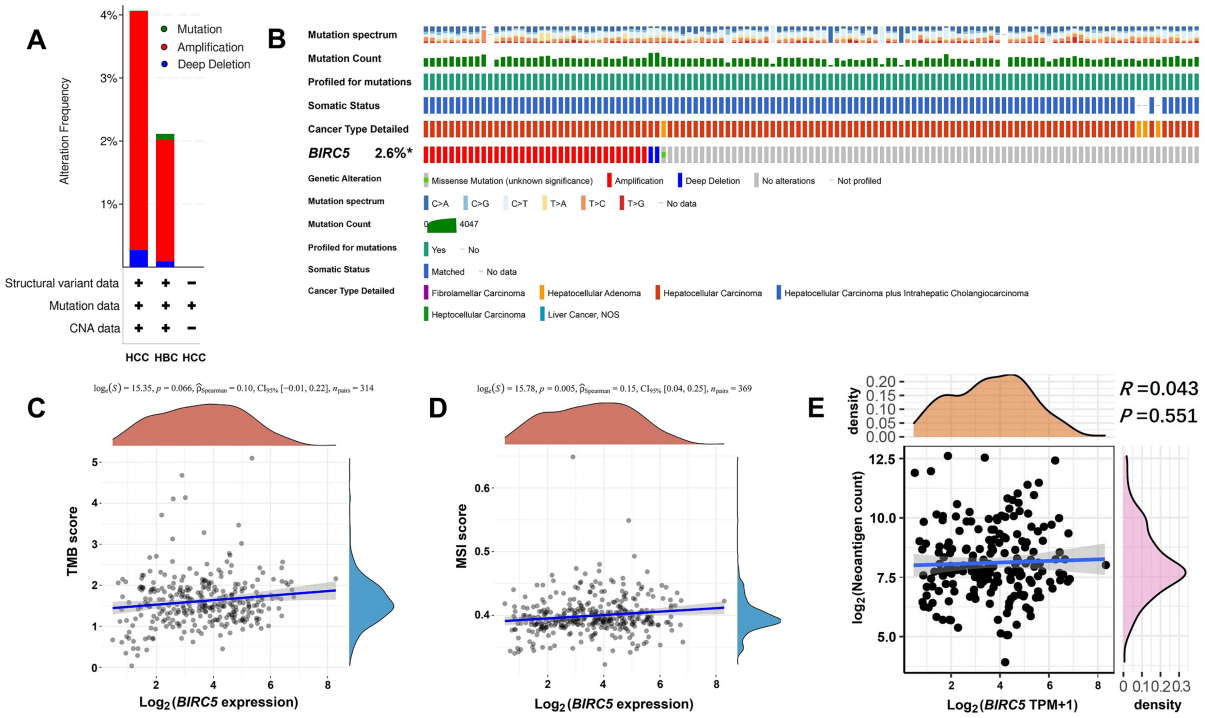

Figure 11. (A and B) Genetic alteration detection of *BIRC5* from the cBioPortal database; (C-E) The correlation between *BIRC5* and TMB score, MSI score, and neoantigen, respectively. TMB: Tumor mutational burden; MSI: microsatellite instability.

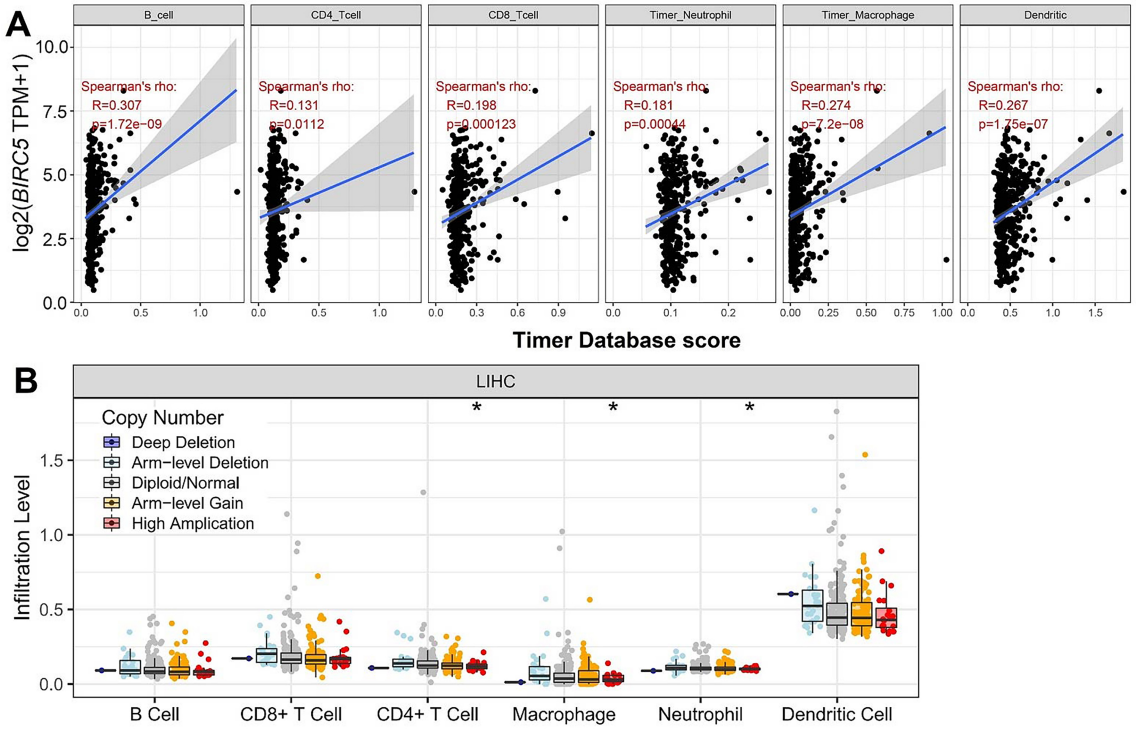

Figure 12. The expression of *BIRC5* in immune cell infiltration. (A) The relationship between *BIRC5* and six different levels of immune cell infiltration; (B) Six immune cell infiltration levels in terms of copy number (the copy number contains deep deletion, arm-level deletion, diploid/normal, arm-level gain, and high amplification).

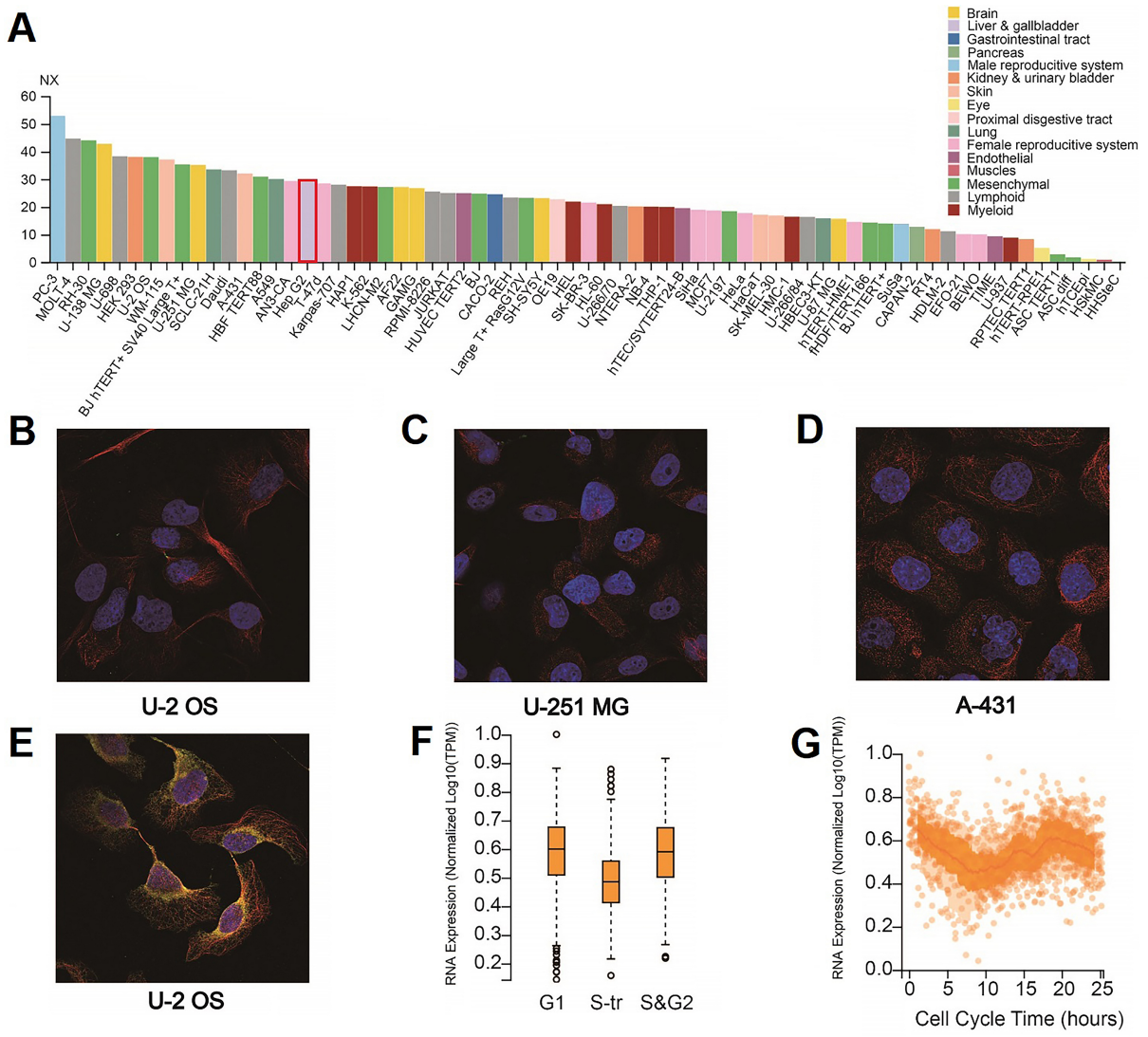

Figure 13. (A) The RNA expression of Hep-G2 in the liver was derived from the "RNA EXPRESSION" module of the HPA database; (B-E) Subcellular location of *BIRC5* was evaluated at multiple levels, revealing its presence in the cancer cell cytoplasm and nuclei; (F and G) The levels of *BIRC5* expression in liver cell cycle. HPA: Human Protein Atlas; OS: overall survival; U-251MG: human astrocytoma cells.

influenced by the activation of the PI3K/AKT signaling pathway, which inhibits autophagic cell death during HCC progression[46,47]. Additionally, *BIRC5* was induced by IGF-1 signaling, promoting epithelial-mesenchymal transition[48,49]. The prognostic relevance of OS-, DFS-, PFS-, and DSS-related prognostic signatures in HCC was further evaluated using univariate Cox regression and LASSO Cox regression analyses. Based on the coefficient scores, *BIRC5* emerged as a potential prognostic signature. Further screening through univariate and multivariate Cox analyses confirmed BIRC5 as an independent risk factor when combined with predictive signatures and clinical parameters. Subsequently, nomograms were constructed to predict OS, DFS, PFS, and DSS in HCC patients, demonstrating good concordance between the predicted and actual survival outcomes. Furthermore, validation using external ICGC cohorts, based on the same risk score model derived from the TCGA training cohort, revealed that *TP53*, *ARSA*, *ATIC*, *GAPDH*, *BIRC5*, and *CDKN2A* were strongly associated with poor HCC prognosis. Kaplan-Meier survival analysis with the log-rank test indicated that patients with high *BIRC5* expression had significantly worse clinical outcomes compared to those with low *BIRC5* expression. Additionally, ROC analysis demonstrated

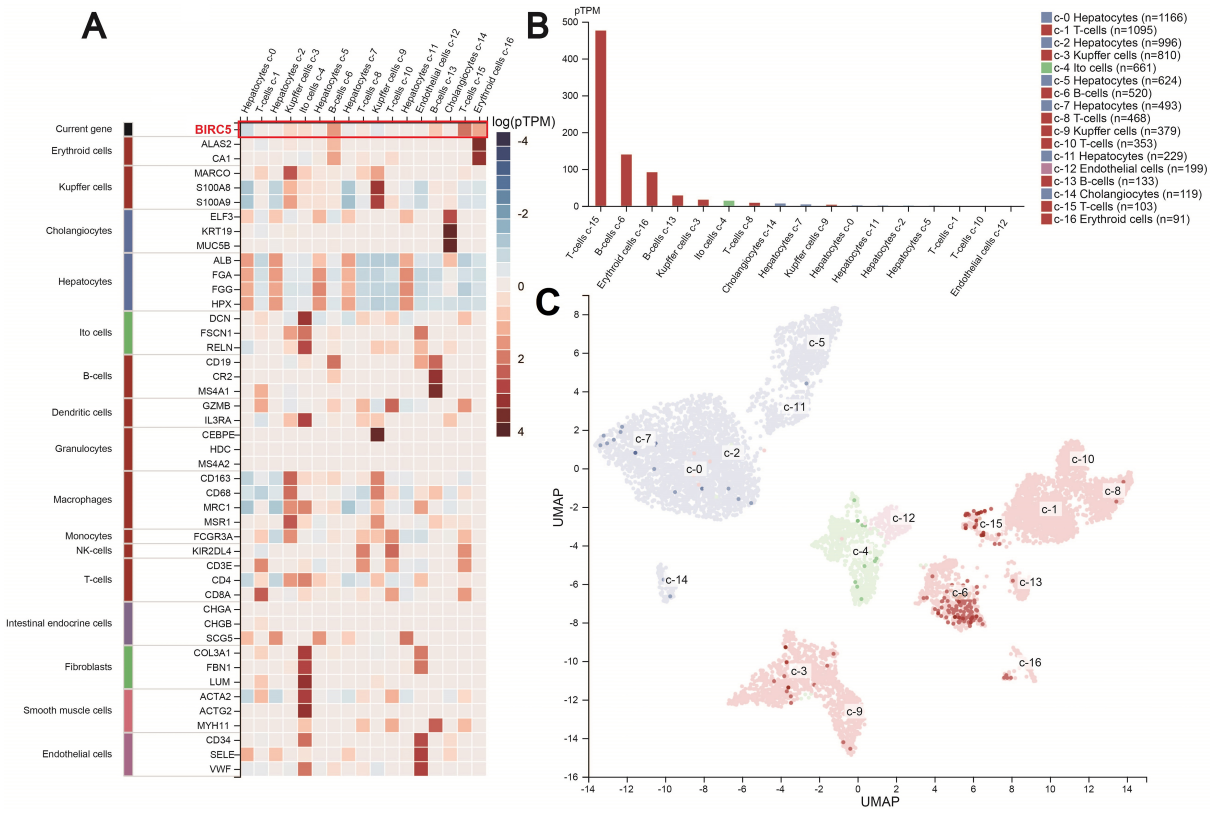

Figure 14. (A-C) The RNA expression of *BIRC5* in the single cell type clusters identified in the HPA database. HPA: Human Protein Atlas.

excellent predictive performance across multiple survival time points. In conclusion, through training and validation models, *BIRC5* was identified as an independent prognostic signature for HCC.

BIRC5 is a crucial member of the apoptosis-inhibiting gene family, playing a key role in encoding regulatory molecules that suppress cell apoptosis[5,28]. Based on the above analysis, six models were constructed to investigate the impact of *BIRC5* on the OS of patients infected with hepatitis B and C. Interestingly, low *BIRC5* expression was associated with better clinical outcomes, leading to a reduction in hepatitis B and C patient mortality. In HCC tissues, *BIRC5* expression was significantly higher than in healthy controls. *BIRC5* not only promotes cell proliferation and invasion but also inhibits apoptosis and cycle arrest[50]. It plays a critical role in regulating cancer cell autophagy, contributing to chemotherapy and radiotherapy resistance, and accelerating metastasis and recurrence, all of which support cancer cell survival and tumor maintenance[51]. Additionally, BIRC5 serves as a negative regulator of apoptosis[12,17,52]. Regarding tumor angiogenesis, *BIRC5* enhances the expression of VEGF, which, in turn, promotes angiogenesis in the tumor stroma[53]. Liu *et al.* reported that *BIRC5* may play an essential part in the IGF-1 signaling pathway by regulating epithelial-mesenchymal transition (EMT) in HCC[49]. Notably, IHC analysis revealed that *BIRC5* protein expression was moderately elevated in HCC compared to normal tissues, as indicated by cytoplasmic immunoreactivity. The study identified significant survival differences among patients with varying clinical characteristics. HCC cells acquire aggressive properties through a series of genomic changes[54,55]. Among 369 HCC patients, 3.79% exhibited gene amplification, 0.27% had deep deletions, and 2.7% carried other genetic alterations. Surprisingly, the mutation spectrum, cancer type details, and somatic status showed nearly 100% occurrence in HCC samples. *BIRC5* appears to promote tumor growth in the HCC microenvironment, given its positive correlation with TMB, MSI, and neoantigen presence. According

to Xiao *et al.*, a new predictive score incorporating *BIRC5* as a key component identified various tumor-infiltrating immune cells (TIICs) in HCC[56]. TIICs potentially contribute to tumor progression[57] and are predominantly enriched and clonally amplified in HCC [58]. Their accumulation is also linked to poor prognosis[59-61]. *BIRC5* was significantly associated with the abundance of six types of TIICs, suggesting its potential as a diagnostic biomarker for HCC and its involvement in immune regulation. Furthermore, high *BIRC5* amplification was frequently observed in immune infiltrates, such as CD4 T cells, macrophages, and neutrophils. The "SINGLE CELL TYPE" analysis showed that *BIRC5* is highly expressed in 16 different cell types, particularly in T cells, erythroid cells, and B cells in the liver. *BIRC5* expression levels were also examined in Hep-G2 cells, indicating that *BIRC5* immunostaining was mainly localized in the cytoplasm and nuclei of cancer cells. Additionally, variations in *BIRC5* transcript expression were strongly correlated with the cell cycle, potentially influencing the progression of the HCC cell cycle.

The relationship between the *BIRC5* and HCC diagnosis and clinical treatment has garnered significant attention in recent research. *BIRC5*, also known as Survivin, is a member of the inhibitor of apoptosis protein (IAP) family and plays a crucial role in regulating cell survival, proliferation, and apoptosis. Its abnormal expression contributes to HCC tumorigenesis by promoting cancer cell proliferation and inhibiting apoptosis[62,63]. In terms of diagnosis, *BIRC5* has shown potential as a biomarker for HCC, facilitating early detection and prognosis assessment. However, further validation in larger patient cohorts is required. *BIRC5* expression levels correlate with tumor size, metastasis, and patient survival, making it a promising target for diagnostic applications. Clinically, *BIRC5*-targeted therapies, such as small molecule inhibitors and immunotherapies, are being explored as potential treatments to inhibit tumor growth and improve patient outcomes. The underlying mechanisms of *BIRC5* in HCC involve its interaction with key signaling pathways, including the PI3K/AKT and NF-κB pathways, which regulate apoptosis and cell cycle progression. Understanding these mechanisms could provide valuable insights into novel therapeutic strategies for HCC.

The study has several limitations as follows: Firstly, it employs a descriptive study design, which cannot completely eliminate the influence of confounding factors; Secondly, the study may be limited by a small sample size, especially for specific patient groups (e.g., those with HBV or HCV infections), which could affect the generalizability of the conclusions; Thirdly, autophagy is a multifaceted and complex biological process, and a single biomarker may not fully capture its role in HCC. Future studies should comprehensively investigate the complex effects of autophagy on the prognosis of HBV/HCV-infected patients.

In conclusion, this study systematically integrates publicly available sequencing data with clinically validated datasets to establish risk prognostic models for identifying *BIRC5* as a key prognostic signature. *BIRC5* could effectively and independently predict the OS, PFS, DFS, and DSS in HCC patients. Importantly, the identification of *BIRC5* as a prognostic factor provides a basis for the development of therapeutic interventions for HCC via autophagy-related mechanisms.

DECLARATIONS

Acknowledgments

The authors thank those who participated in the preparation and maintenance of the databases used in this study, and the School of Public Health, Shaanxi University of Chinese Medicine, for assistance.

Authors' contributions

Conceived and designed the study: Li J, Zhang R
Performed bioinformatics analysis and experiments: Wang R
Wrote the manuscript: Guo H, Kou X
Reviewed and approved the final manuscript: Wang R, Guo H, Kou X, Chen R, Zhang R, Li J

Availability of data and materials

The TCGA and ICGC datasets were obtained from open databases. TCGA dataset can be obtained from the following website: http://cancergenome.nih.gov. ICGC dataset can be obtained from the data portal: https://dcc.icgc.org/. Additional raw data will be made available by the corresponding authors upon reasonable request.

Financial support and sponsorship

Project supported by the National Natural Science Foundation of China (Grant NO.82174330, 82374418); Shaanxi Provincial Department of Science and Technology Innovation Team Program (2022TD-55); Shaanxi Provincial Administration of Traditional Chinese Medicine Innovation Team Program (2022-SLRH-LJ-002); Shaanxi University of Traditional Chinese Medicine High-level Chinese Medicine Key Discipline Construction Program (2024XKZD19); Shaanxi Provincial Administration of Traditional Chinese Medicine Key Research Laboratory Program.

Conflicts of interest

All authors declared that there are no conflicts of interest.

Ethics approval and consent to participate

All data for this study are derived from publicly available databases and do not directly involve human participants. Therefore, ethical approval was not required for this article.

Consent for publication

Not applicable.

REFERENCES

1. Sung H, Ferlay J, Siegel RL, et al. Global cancer statistics 2020: GLOBOCAN estimates of incidence and mortality worldwide for 36 cancers in 185 countries. *CA Cancer J Clin.* 2021;71:209-49. DOI PubMed
2. Villanueva A. Hepatocellular carcinoma. *N Engl J Med.* 2019;380:1450-62. DOI PubMed
3. Wang W, Wei C. Advances in the early diagnosis of hepatocellular carcinoma. *Genes Dis.* 2020;7:308-19. DOI PubMed PMC
4. Luo YD, Yu HQ, Liu XY, et al. Prognostic and predicted significance of Ubqln2 in patients with hepatocellular carcinoma. *Cancer Med.* 2020;9:4083-94. DOI PubMed PMC
5. Feng R, Li J, Xuan W, Liu H, Cheng D, Wang G. An autophagy-related gene-based prognostic risk signature for hepatocellular carcinoma: construction and validation. *Comput Math Methods Med.* 2021;2021:5770228. DOI PubMed PMC
6. Li X, Xu W, Kang W, et al. Genomic analysis of liver cancer unveils novel driver genes and distinct prognostic features. *Theranostics.* 2018;8:1740-51. DOI PubMed PMC
7. Liang JY, Wang DS, Lin HC, et al. A novel ferroptosis-related gene signature for overall survival prediction in patients with hepatocellular carcinoma. *Int J Biol Sci.* 2020;16:2430-41. DOI PubMed PMC
8. Ouyang G, Yi B, Pan G, Chen X. A robust twelve-gene signature for prognosis prediction of hepatocellular carcinoma. *Cancer Cell Int.* 2020;20:207. DOI PubMed PMC
9. Kim E, Viatour P. Hepatocellular carcinoma: old friends and new tricks. *Exp Mol Med.* 2020;52:1898-907. DOI PubMed PMC
10. Yang W, Niu L, Zhao X, et al. Development and validation of a survival model based on autophagy-associated genes for predicting prognosis of hepatocellular carcinoma. *Am J Transl Res.* 2020;12:6705-22. DOI
11. Yang Y, Yao JH, Du QY, et al. Connexin 32 downregulation is critical for chemoresistance in oxaliplatin-resistant HCC cells

associated with EMT. *Cancer Manag Res.* 2019;11:5133-46. DOI PubMed PMC

12. Zhu Y, Wang R, Chen W, Chen Q, Zhou J. Construction of a prognosis-predicting model based on autophagy-related genes for hepatocellular carcinoma (HCC) patients. *Aging.* 2020;12:14582-92. DOI PubMed PMC
13. Liang TT, Shao Q, Deng ZC, Wang T, Kang QZ. Systemic expression analysis reveals prognostic significance of WIPI3 in hepatocellular carcinoma. *Front Genet.* 2020;11:847. DOI PubMed PMC
14. Liu L, Liao JZ, He XX, Li PY. The role of autophagy in hepatocellular carcinoma: friend or foe. *Oncotarget.* 2017;8:57707-22. DOI PubMed PMC
15. Huang F, Wang BR, Wang YG. Role of autophagy in tumorigenesis, metastasis, targeted therapy and drug resistance of hepatocellular carcinoma. *World J Gastroenterol.* 2018;24:4643-51. DOI PubMed PMC
16. Fang Q, Chen H. Development of a novel autophagy-related prognostic signature and nomogram for hepatocellular carcinoma. *Front Oncol.* 2020;10:591356. DOI PubMed PMC
17. Xu W, Guo W, Lu P, Ma D, Liu L, Yu F. Identification of an autophagy-related gene signature predicting overall survival for hepatocellular carcinoma. *Biosci Rep.* 2021;41:BSR20203231. DOI PubMed PMC
18. Fang S, Su J, Liang B, et al. Suppression of autophagy by mycophenolic acid contributes to inhibition of HCV replication in human hepatoma cells. *Sci Rep.* 2017;7:44039. DOI PubMed PMC
19. Xiong X, Wu M, Zhang H, et al. Atg5 siRNA inhibits autophagy and enhances norcantharidin-induced apoptosis in hepatocellular carcinoma. *Int J Oncol.* 2015;47:1321-8. DOI PubMed
20. Ni HM, Woolbright BL, Williams J, et al. Nrf2 promotes the development of fibrosis and tumorigenesis in mice with defective hepatic autophagy. *J Hepatol.* 2014;61:617-25. DOI PubMed PMC
21. Pan J, Lu C, Jun W, et al. The up-regulation of P62 levels is associated with resistance of sorafenib in hepatocarcinoma cells. *Int J Clin Exp Pathol.* 2019;12:2622-30. PubMed PMC
22. Gu Y, Li P, Peng F, et al. Autophagy-related prognostic signature for breast cancer. *Mol Carcinog.* 2016;55:292-9. DOI PubMed
23. Ko YH, Cho YS, Won HS, et al. Prognostic significance of autophagy-related protein expression in resected pancreatic ductal adenocarcinoma. *Pancreas.* 2013;42:829-35. DOI PubMed
24. Zhang H, Lu X, Wang N, et al. Autophagy-related gene expression is an independent prognostic indicator of glioma. *Oncotarget.* 2017;8:60987-1000. DOI PubMed PMC
25. Association for the Study of the Liver. EASL clinical practice guidelines: management of hepatocellular carcinoma. *J Hepatol.* 2018;69:182-236. DOI PubMed
26. Wang Z, Jensen MA, Zenklusen JC. A practical guide to the cancer genome atlas (TCGA). In: Mathé E, Davis S, Editors. Statistical genomics. New York: Springer; 2016. pp. 111-41. DOI PubMed
27. Li C, Wu ZH, Yuan K. Autophagy-related signature for head and neck squamous cell carcinoma. *Dis Markers.* 2020;2020:8899337. DOI PubMed PMC
28. Zhang J, Zhang M, Huang J, et al. Development and validation of an autophagy-related gene signature for predicting the prognosis of hepatocellular carcinoma. *Biomed Res Int.* 2021;2021:7771037. DOI PubMed PMC
29. Doncheva NT, Morris JH, Gorodkin J, Jensen LJ. Cytoscape stringApp: network analysis and visualization of proteomics data. *J Proteome Res.* 2019;18:623-32. DOI PubMed PMC
30. Xu YY, Zhou H, Murphy RF, Shen HB. Consistency and variation of protein subcellular location annotations. *Proteins.* 2021;89:242-50. DOI PubMed PMC
31. Lin S, Zheng L, Lu Y, Xia Q, Zhou P, Liu Z. Comprehensive analysis on the expression levels and prognostic values of LOX family genes in kidney renal clear cell carcinoma. *Cancer Med.* 2020;9:8624-38. DOI PubMed PMC
32. Lv J, Zhu Y, Ji A, Zhang Q, Liao G. Mining TCGA database for tumor mutation burden and their clinical significance in bladder cancer. *Biosci Rep.* 2020;40:BSR20194337. DOI PubMed PMC
33. Ott PA, Hu Z, Keskin DB, et al. An immunogenic personal neoantigen vaccine for patients with melanoma. *Nature.* 2017;547:217-21. DOI PubMed PMC
34. Hu J, Qiu D, Yu A, et al. YTHDF1 is a potential pan-cancer biomarker for prognosis and immunotherapy. *Front Oncol.* 2021;11:607224. DOI PubMed PMC
35. Liu J, Chen Z, Zhao P, Li W. Prognostic and immune regulating roles of YIF1B in Pan-cancer: a potential target for both survival and therapy response evaluation. *Biosci Rep.* 2020;40:BSR20201384. DOI PubMed PMC
36. Li T, Fu J, Zeng Z, et al. TIMER2.0 for analysis of tumor-infiltrating immune cells. *Nucleic Acids Res.* 2020;48:W509-14. DOI PubMed PMC
37. Zhang Z, Zhang Y, Mo W. The autophagy related gene CHAF1B is a relevant prognostic and diagnostic biomarker in hepatocellular carcinoma. *Front Oncol.* 2020;10:626175. DOI PubMed PMC
38. Lin Z, Niu Y, Wan A, et al. RNA m^6A methylation regulates sorafenib resistance in liver cancer through FOXO3-mediated autophagy. *EMBO J.* 2020;39:e103181. DOI PubMed PMC
39. Lu X, Paliogiannis P, Calvisi DF, Chen X. Role of the mammalian target of rapamycin pathway in liver cancer: from molecular genetics to targeted therapies. *Hepatology.* 2021;73:49-61. DOI PubMed PMC
40. Wei Q, Zhu R, Zhu J, Zhao R, Li M. E2-induced activation of the NLRP3 inflammasome triggers pyroptosis and inhibits autophagy in HCC cells. *Oncol Res.* 2019;27:827-34. DOI PubMed PMC
41. Huo X, Qi J, Huang K, et al. Identification of an autophagy-related gene signature that can improve prognosis of hepatocellular

carcinoma patients. *BMC Cancer.* 2020;20:771. DOI PubMed PMC

42. Fan Q, Yang L, Zhang X, et al. Autophagy promotes metastasis and glycolysis by upregulating MCT1 expression and Wnt/β-catenin signaling pathway activation in hepatocellular carcinoma cells. *J Exp Clin Cancer Res.* 2018;37:9. DOI PubMed PMC
43. Li J, Yang B, Zhou Q, et al. Autophagy promotes hepatocellular carcinoma cell invasion through activation of epithelial-mesenchymal transition. *Carcinogenesis.* 2013;34:1343-51. DOI
44. Deng G, Zeng S, Qu Y, et al. BMP4 promotes hepatocellular carcinoma proliferation by autophagy activation through JNK1-mediated Bcl-2 phosphorylation. *J Exp Clin Cancer Res.* 2018;37:156. DOI PubMed PMC
45. Song Z, Zhang G, Yu Y, Li S. A prognostic autophagy-related gene pair signature and small-molecule drugs for hepatocellular carcinoma. *Front Genet.* 2021;12:689801. DOI PubMed PMC
46. Wei Y, Chen X, Liang C, et al. A noncoding regulatory RNAs network driven by Circ-CDYL acts specifically in the early stages hepatocellular carcinoma. *Hepatology.* 2020;71:130-47. DOI PubMed
47. Roca H, Varsos Z, Pienta KJ. CCL2 protects prostate cancer PC3 cells from autophagic death via phosphatidylinositol 3-kinase/AKT-dependent survivin up-regulation. *J Biol Chem.* 2008;283:25057-73. DOI PubMed PMC
48. Peng Y, Liu C, Li M, et al. Identification of a prognostic and therapeutic immune signature associated with hepatocellular carcinoma. *Cancer Cell Int.* 2021;21:98. DOI PubMed PMC
49. Liu F, Sun Y, Liu B, et al. Insulin-like growth factor-1 induces epithelial-mesenchymal transition in hepatocellular carcinoma by activating survivin. *Oncol Rep.* 2018;40:952-8. DOI PubMed
50. Su C. Survivin in survival of hepatocellular carcinoma. *Cancer Lett.* 2016;379:184-90. DOI PubMed
51. Cao L, Li C, Shen S, et al. OCT4 increases BIRC5 and CCND1 expression and promotes cancer progression in hepatocellular carcinoma. *BMC Cancer.* 2013;13:82. DOI PubMed PMC
52. Xu M, Hu X, Zhang M, Ge Y. What is the impact of BIRC5 gene polymorphisms on urinary cancer susceptibility? *Gene.* 2020;733:144268. DOI PubMed
53. Fernández JG, Rodríguez DA, Valenzuela M, et al. Survivin expression promotes VEGF-induced tumor angiogenesis via PI3K/Akt enhanced β-catenin/Tcf-Lef dependent transcription. *Mol Cancer.* 2014;13:209. DOI PubMed PMC
54. Cao D, Chen MK, Zhang QF, et al. Identification of immunological subtypes of hepatocellular carcinoma with expression profiling of immune-modulating genes. *Aging.* 2020;12:12187-205. DOI PubMed PMC
55. Dong LY, Zhou WZ, Ni JW, et al. Identifying the optimal gene and gene set in hepatocellular carcinoma based on differential expression and differential co-expression algorithm. *Oncol Rep.* 2017;37:1066-74. DOI PubMed
56. Xiao H, Wang B, Xiong HX, et al. A novel prognostic index of hepatocellular carcinoma based on immunogenomic landscape analysis. *J Cell Physiol.* 2021;236:2572-91. DOI PubMed
57. Domingues P, González-Tablas M, Otero Á, et al. Tumor infiltrating immune cells in gliomas and meningiomas. *Brain Behav Immun.* 2016;53:1-15. DOI PubMed
58. Zheng C, Zheng L, Yoo JK, et al. Landscape of infiltrating T cells in liver cancer revealed by single-cell sequencing. *Cell.* 2017;169:1342-56.e16. DOI PubMed
59. Sun H, Liu L, Huang Q, et al. Accumulation of tumor-infiltrating CD49a^{+} NK cells correlates with poor prognosis for human hepatocellular carcinoma. *Cancer Immunol Res.* 2019;7:1535-46. DOI PubMed
60. Pourbagheri-Sigaroodi A, Fallah F, Bashash D, Karimi A. Unleashing the potential of gene signatures as prognostic and predictive tools: a step closer to personalized medicine in hepatocellular carcinoma (HCC). *Cell Biochem Funct.* 2024;42:e3913. DOI PubMed
61. Zhou Y, Shan R, Xie W, et al. Role of autophagy-related genes in liver cancer prognosis. *Genomics.* 2024;116:110852. DOI PubMed
62. Zhang H, Xia P, Liu J, Chen Z, Ma W, Yuan Y. ATIC inhibits autophagy in hepatocellular cancer through the AKT/FOXO3 pathway and serves as a prognostic signature for modeling patient survival. *Int J Biol Sci.* 2021;17:4442-58. DOI PubMed PMC
63. Liu Y, Chen X, Luo W, et al. Identification and validation of Birc5 as a novel activated cell cycle program biomarker associated with infiltration of immunosuppressive myeloid-derived suppressor cells in hepatocellular carcinoma. *Cancer Med.* 2023;12:16370-85. DOI PubMed PMC